



REVIEW

A Review of Basic Mechanical Properties of Bamboo Scrimber Based on Small-Scale Specimens

Xin Xue^{1,2,3}, Haitao Li^{1,2,3,*} and Rodolfo Lorenzo⁴

¹College of Civil Engineering, Nanjing Forestry University, Nanjing, 210037, China

²National-Provincial Joint Engineering Research Center of Biomaterials for MACHINERY PACKAGE, Nanjing Forestry University, Nanjing, 210037, China

³Jiangsu Engineering Research Center of Bamboo and Wood Carbon Fixation Materials and Structures, Nanjing Forestry University, Nanjing, 210037, China

⁴Department of Civil, Environmental and Geomatic Engineering, University College London, London, WC1E 6BT, UK

*Corresponding Author: Haitao Li. Email: lhaitao1982@126.com

Received: 28 February 2023 Accepted: 02 January 2024 Published: 12 June 2024

ABSTRACT

This review summarizes the existing knowledge about the mechanical properties of bamboo scrimber (BS) in literature. According to literature reviews, the strength of BS under different load modes is affected by a series of factors, such as the type of original bamboo, growth position, resin content, treatment method and density. Therefore, different production processes can be adopted according to different requirements, and bamboo scrimbers can also be classified accordingly. In addition, this review summarizes the changes in different factors considered by scholars in the research on the mechanical properties of BS, so that readers can have an overall understanding of the existing research and make more innovative and valuable research on this basis. This review provides and discusses the conclusive observations, the current research gaps and future research directions on the mechanical properties of BS.

KEYWORDS

Bamboo scrimber; manufacturing process; mechanical properties; failure modes; constitutive model

1 Introduction

With the proposal of the concept of green development and sustainable development, the application of natural green materials is paid more and more attention in the engineering field. Wood structure has been applied in the field of modern architecture earlier, and now the research on wood structure is more in-depth. It is no longer just limited to the study of wood properties, but has a deeper exploration of the overall performance of wood structures [1,2].

Bamboo is also an important ecological and cultural resource. China is known as the “Kingdom of Bamboo”, and the output of bamboo ranks first in the world. However, although the original bamboo has good toughness and texture, it also has some disadvantages, such as large differences in mechanical properties. Therefore, in order to make better use of the advantages of bamboo, in today’s industrialized world, raw bamboo is usually processed and produced as various bamboo composites. Nowadays, as



more and more attention is paid to the application of bamboo, there is more research on bamboo and bamboo composites, and the theories are more in-depth, micro- and macro-properties and chemical characterization have been extensively studied, micro- and macro-properties [3–6] and chemical characterization [7–9] have been extensively studied; Bamboo and bamboo composite materials have been applied in the construction field [10].

Bamboo scrimber (abbreviated as BS) is a wood-like material made of bamboo. It is inspired by reconstituted wood, with excellent integrity, high strength, high density, high stiffness and good stability [11,12]. It was initiated in the 1970s and has been well-developed and applied now [13–15]. The production process of BS (as shown in Fig. 1) is roughly divided into: raw bamboo, truncation, radial splitting, removing the bamboo outer layer and bamboo inner layer, defibering, drying, dipping, putting into the mold, hot-or cold-pressing [16]. In addition, at different stages of production, there are different factors affecting the properties of the final produced BS, such as the type of raw bamboo [17–21], the treatment method of bamboo strips [22–26], the drying temperature and time [27], the concentration of adhesive [28–30] and the pressing process [31–35].

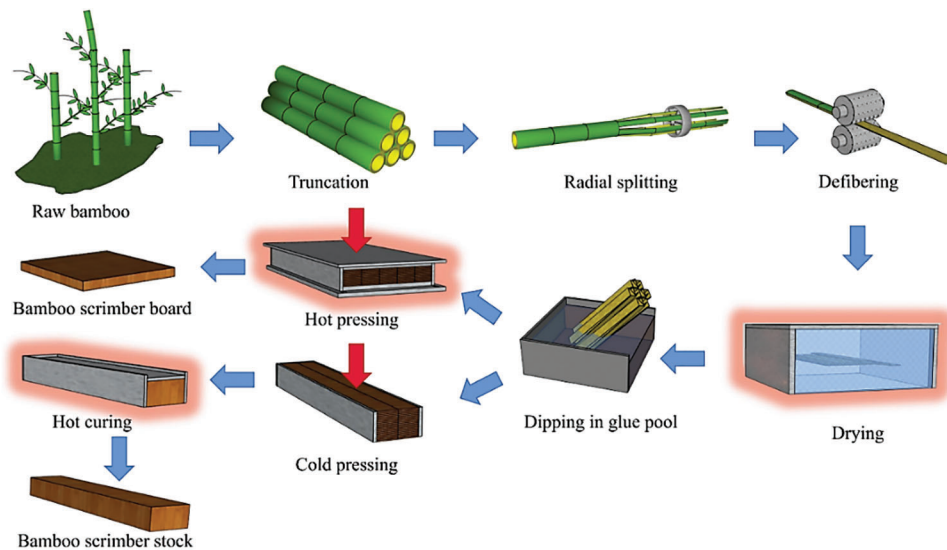


Figure 1: Manufacturing process

In the early manufacturing of BS, the raw materials are mainly waste bamboo silk or bamboo strips that remove the bamboo outer layer and bamboo inner layer, which makes the utilization rate of bamboo not high. In view of this situation, the Wood Industry Research Institute of Chinese Academy of Forestry has developed a bamboo treatment technology without removing the bamboo outer layer and bamboo inner layer, which makes the primary utilization rate of bamboo up to more than 90%, which is a major breakthrough in the field of bamboo processing and application [36]. As a result, BS has been well used in the field of building materials due to its efficient utilization of bamboo and excellent mechanical properties.

Researches have shown that BS has better mechanical properties than wood, engineering wood and engineering bamboo [37–39]. However, the size of BS is limited by the manufacturing process, which restricts the application of BS in the field of construction engineering to a certain extent. As BS is a kind of material made from raw bamboo through a series of processing and belongs to combustible material, the research on fire resistance is also an important aspect [40,41]. At the same time, high nutrition and

moisture in bamboo will lead to moth decay, so the research on the anti-corrosion performance of raw bamboo and BS should not be ignored [42–45]. This review focuses on the existing research on the mechanical properties of BS, and puts forward the problems that need further research or different assumptions on the research methods, in order to provide new ideas for the design and application of BS.

2 Investigation of Literature

The number of studies on bamboo scrimber was counted through ScienceDirect database and CNKI database. The research named “Chong Zuzhu” is mainly screened from CNKI database, while the research named “bamboo scribe” and “parallel bamboo strand lumber” are screened from science direct database, respectively. The literature types searched are mainly academic journals, dissertations and conference papers. The statistical results are shown in Fig. 2.

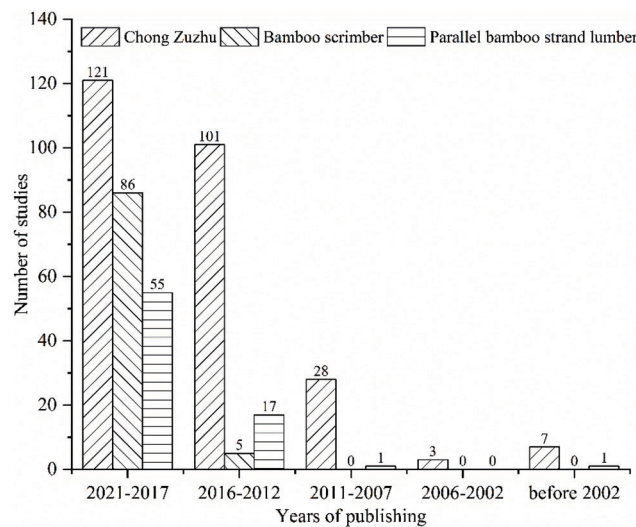


Figure 2: Statistical results

This review mainly summarizes the mechanical properties of BS, and discusses the compressive, tensile, shear and bending properties of BS. The selected literature on the mechanical properties of BS is summarized in Tables 1–4.

Table 1: Literature on compressive properties

Compression							
Study	Species	Origin	Glue	Size (mm)	Method	standard	Strength (MPa)
Li et al. [20]	<i>Phyllostachys pubescens</i>	China	–	–	Hot pressed	GB/T 1934–1935–2009	II: 73.46 ⊥: 12.75–21.95
Gong et al. [21]	<i>Neosinocalamus affinis</i>	China	PF	30 × 20 × 20	Hot pressed	GB/T 1935–2009	II: 104.82
Zhang et al. [46]	<i>Bambusa emeiensis</i>	China	–	30 × 20 × 20	–	GB/T 1935–2009 GB/T 1939–2009	II: 129.17 ⊥: 40.19–45.5
Li [47]	<i>Phyllostachys pubescens</i>	China	–	200 × 50 × 50	Hot pressed	ASTM D143–09	II: 65.5
Li et al. [48]	<i>Phyllostachys pubescens</i>	China	PF	150 × 50 × 50	–	–	II: 100.9 ⊥: 52.8

(Continued)

Table 1 (continued)

Study	Species	Origin	Glue	Compression			
				Size (mm)	Method	standard	Strength (MPa)
Wei et al. [49]	–	China	PF	150 × 50 × 50	Cold pressed	GB/T 1927–1991	II: 85.1
Sharma et al. [50]	<i>Phyllostachys pubescens</i>	China	PF	60 × 20 × 20 50 × 50 × 50	–	ASTM D143–09	II: 86 ⊥: 37
Li et al. [51]	<i>Phyllostachys pubescens</i>	China	–	100 × 100 × 100	–	GB/T 50329–2012	II: 61.8–71.1 ⊥: 18.8–27.2
Chen et al. [52]	–	China	–	120 × 25 × 25	Cold pressed	ASTM D143–09	–
Wei et al. [53]	–	China	–	120 × 25 × 25	Hot pressed	ASTM D143–94 (2000)	–
Li et al. [54]	<i>Phyllostachys pubescens</i>	China	–	200 × 28 × 28	–	ASTM D143–94 (2000) GB 1927–1943–91	–
Kumar et al. [55]	<i>Phyllostachys pubescens</i>	China	PF	30 × 20 × 20	Cold pressed	ČSN490110–ČSN490112	II: 104.71–115.7 ⊥: 49.33–77
Wang et al. [56]	<i>Phyllostachys pubescens</i>	China	PF	30 × 20 × 20	Hot pressed	GB/T 1935–2009 GB/T 15777–2017	II: 94.67 ⊥: 45.85–48.8
Li et al. [57]	<i>Phyllostachys pubescens</i>	China	PF	30 × 20 × 20	Hot pressed	GB/T 40247–2021	II: 127.33 ⊥: 72.96
Sylvayanti et al. [58]	<i>Gigantochloa</i>	Indonesia	PF	200 × 30 × 30 150 × 30 × 30	Cold pressed	ASTM D143–14	II: 64.85 ⊥: 19.6
Wu et al. [59]	<i>Phyllostachys pubescens</i>	China	PF	30 × 20 × 20	Hot pressed	ASTM D143–14	II: 129.25 ⊥: 65.77–73.34
Chen et al. [60]	–	China	–	150 to 1200 × 50 × 50 150 to 1200 × 100 × 100 150 to 900 × 75 × 50 150 to 1200 × 100 × 50	Cold pressed	GB/T 1935–2009 GB/T 50329–2012	II: 84.4
Rao et al. [61]	<i>Bambusa chungii</i>	China	PF	60 × 13 × 13	Hot pressed	GB/T 17657–2013	–
Sewar et al. [62]	<i>Phyllostachys pubescens</i>	China	PF	100 × 25 × 25	Hot pressed	BS 373–2018	II: 121 ⊥: 60.5
Hu et al. [63]	<i>Phyllostachys pubescens</i>	China	PF	60 × 20 × 20	Hot pressed	GB/T 30364	–
Zheng et al. [64]	<i>Neosinocalamus affinis</i>	China	PF	30 × 20 × 20	Hot pressed	GB/T 1935–2009 ASTM D143–14	II: 132.4
Wu et al. [65]	–	China	Epoxy	Height: 205 to 400, Diameter: 68 to 133	Hot pressed	ASTM D143–09	II: 112.01
Yu et al. [66]	<i>Phyllostachys pubescens</i>	China	PF	30 × 20 × 20	Hot pressed	GB/T 1935–2009	II: 87.5–100.7
Chen et al. [67]	–	China	–	210 × 70 × 70	–	GB/T 50329–2012	II: 65.5
Rao et al. [68]	<i>Phyllostachys pubescens</i>	China	PF	60 × 13 × 13	Hot pressed	GB/T 30364–2013 GB/T 17657–2013 GB/T 20241–2006	II: 106.68
Li et al. [69]	<i>Phyllostachys pubescens</i>	China	PF	100 to 200 × 50 × 50	Hot pressed	GB/T 50329–2012	II: 96.3–102.1 ⊥: 49.1–54.4
Wei et al. [70]	–	China	PF	420 × 140 × 140	Cold pressed	ASTM D143–09	II: 85.1, 78.7
Shangguan et al. [71]	<i>Neosinocalamus affinis</i>	China	PF	30 × 20 × 20	Hot pressed	GB 1935–2009 ASTM D143–2009	II: 133.4 ⊥: 25.7
Xu et al. [72]	<i>Phyllostachys pubescens</i>	China	PF	100 × 25 × 25	–	ASTM D143–14	II: 5.32–66.54 ⊥: 0.56–28.01

(Continued)

Table 1 (continued)

Compression							
Study	Species	Origin	Glue	Size (mm)	Method	standard	Strength (MPa)
Huang et al. [73]	<i>Phyllostachys</i>	China	–	200 × 50 × 50	–	ASTM D143-09	∥ : 65.53 ⊥ : 23.14
Yang et al. [74]	<i>Phyllostachys pubescens</i>	China	Epoxy	150 × 60 × 12/14	–	ASTM D143 ASTM C364	∥ : 48–55
Zhao et al. [75]	<i>Phyllostachys pubescens</i>	China	–	30 × 20 × 20, 75 × 50 × 50, 120 × 80 × 80, 165 × 110 × 110, 210 × 140 × 140	–	GB/T 50329-2012 GB/T1935-2009	∥ : 67.4–91.68
Rao et al. [76]	<i>Phyllostachys pubescens</i>	China	PF	60 × 8.6 × 8.6	–	GB/T 17657-2013	∥ : 81.7–103
Sun et al. [77]	<i>Phyllostachys pubescens</i>	China	PF	40 × 25 × 10	Hot pressed	ASTM D1037-2012	–

Note: PF represents phenol formaldehyde resin, ∥ represents parallel to grain, ⊥ represents perpendicular to grain.

Table 2: Literature on bending properties

Bending							
Study	Species	Origin	Glue	Size (mm)	Method	Standard	Strength (MPa)
Li et al. [20]	<i>Phyllostachys pubescens</i>	China	–	–	Hot pressed	GB/T 1936-2009	125.44
Guan et al. [38]	<i>Phyllostachys pubescens</i>	China	PF	300 × 300 × 20	Hot pressed	GB/T 1936-1991	–
Yang et al. [39]	–	China	–	180 × 60 × 15	–	ASTM D143-1994 GB/T 1936-2009	113.79
Li et al. [48]	<i>Phyllostachys pubescens</i>	China	PF	760 × 50 × 15	–	–	144.3
Sharma et al. [50]	<i>Phyllostachys pubescens</i>	China	PF	800 × 40 × 40	–	ASTM D143-09	119
Kumar et al. [55]	<i>Phyllostachys pubescens</i>	China	PF	–	Cold pressed	ČSN490115 ČSN490116	131.83–166.5
Sylvayanti et al. [58]	<i>Gigantochloa</i>	Indonesia	PF	410 × 25 × 25	Cold pressed	ASTM D143-14	71.14
Rao et al. [61]	<i>Bambusa chungii</i>	China	PF	280 × 20 × 13	Hot pressed	GB/T 17657-2013	253.7
Sewar et al. [62]	<i>Phyllostachys pubescens</i>	China	PF	500 × 90 × 20	Hot pressed	GB/T 17657-2013	104.4
Hu et al. [63]	<i>Phyllostachys pubescens</i>	China	PF	450 × 20 × 20	Hot pressed	GB/T 30364	–
Zheng et al. [64]	<i>Neosinocalamus affinis</i>	China	PF	300 × 20 × 20	Hot pressed	GB/T 1936.1-2-2009 ASTM D143-14	236.6
Rao et al. [68]	<i>Phyllostachys pubescens</i>	China	PF	280 × 25 × 13	Hot pressed	GB/T 30364-2013 GB/T 17657-2013 GB/T 20241-2006	178.35

(Continued)

Table 2 (continued)

Bending							
Study	Species	Origin	Glue	Size (mm)	Method	Standard	Strength (MPa)
Yang et al. [74]	<i>Phyllostachys pubescens</i>	China	Epoxy	180 × 60 × 15/17	–	ASTM D143 ASTM C393	111.3–145.8
Rao et al. [76]	<i>Phyllostachys pubescens</i>	China	PF	222 × 25 × 8.6	–	GB/T 17657–2013 GB/T 20241–2006	167–195
Sun et al. [77]	<i>Phyllostachys pubescens</i>	China	PF	250 × 20 × 10	Hot pressed	GB/T 30364–2013 GB17657-2013 ASTM D2344-2016	–
Liu et al. [78]	<i>Phyllostachys pubescens</i>	China	PF	300 × 30 × 18	–	GB/T 1936.1–2009 GB/T 17657-2013	97–466
Chen et al. [79]	–	China	Epoxy	400 to 1000 × 100 × 70	–	ASTM D143-09	–
Qiu et al. [80]	<i>Phyllostachys pubescens</i>	China	PF	760 × 50 × 50	Hot pressed	ASTM D143-2014	10.47–118.06
Zhao et al. [81]	<i>Phyllostachys pubescens</i>	China	UF	330 × 38 × 17	Cold pressed	GBT 1928-2009 GB/T 50329–2012 GB/T 1936.1-2009	39.243–121.865
Zou et al. [82]	<i>Phyllostachys pubescens</i>	China	–	450 × 100 × 14	–	GB/T 17657	102.6–153.1
Wu et al. [83]	<i>Phyllostachys pubescens</i>	China	PF, Epoxy	600 × 30 × 30	–	GB/T 50329-2012	152.68–289.01
Yu et al. [84]	<i>Neosinocalamus affinis</i>	China	PF	360 × 50 × 18	Hot pressed	ASTM D-1037 ASTM D2344	–
Yang et al. [85]	<i>Phyllostachys pubescens</i>	China	PF	320 to 660 × 50 × 50	Hot pressed	ASTM D143-09 ISO 8375:2009-02	104.43–114.14
Qiu et al. [86]	<i>Phyllostachys pubescens</i>	China	PF	300 × 20 × 20	–	–	–
Qiu et al. [87]	–	China	–	300 × 20 × 20	–	–	–
Wang et al. [88]	<i>Phyllostachys pubescens</i>	China	PF	160 × 10 × 10	Hot pressed	LY/T 3194-2020	120.47

Table 3: Literature on tensile properties

Tension							
Study	Species	Origin	Glue	Size (mm)	Method	Standard	Strength (MPa)
Li et al. [20]	<i>Phyllostachys pubescens</i>	China	–	–	Hot pressed	GB/T 1938–2009	II: 112.78 ⊥: 3.726
Gong et al. [21]	<i>Neosinocalamus affinis</i>	China	PF	370 × 20 × 15	Hot pressed	GB/T 1938–2009	II: 170.65
Zhang et al. [46]	<i>Bambusa emeiensis</i>	China	–	370 × 20 × 20	–	GB/T 1938–2009	II: 248.15
Li [47]	<i>Phyllostachys pubescens</i>	China	–	453 × 25 × 50	Hot pressed	ASTM D143–09	II: 118.4
Li et al. [48]	<i>Phyllostachys pubescens</i>	China	PF	453 × 21 × 15 63 × 50 × 50	–	–	II: 156.2 ⊥: 3.88
Wei et al. [49]	–	China	PF	460 × 25 × 10	Cold pressed	GB/T 1927–1991 ASTM D143–09	II: 138.5
Sharma et al. [50]	<i>Phyllostachys pubescens</i>	China	PF	460 × 25 × 25 62 × 50 × 50	–	ASTM D143–09 BS 373	II: 120 ⊥: 3

(Continued)

Table 3 (continued)

Study	Species	Origin	Glue	Tension		Standard	Strength (MPa)
				Size (mm)	Method		
Wei et al. [53]	–	China	–	420 × 25 × 10	Hot pressed	ASTMD143–94 (2000) GB/T1928–2009	–
Li et al. [54]	<i>Phyllostachys pubescens</i>	China	–	630 × 50 × 50	–	ASTMD143–94 (2000) GB 1927–1943–91 GB/T 50329–2012 GB/T 1938–2009	–
Kumar et al. [55]	<i>Phyllostachys pubescens</i>	China	PF	350 × 20 × 20 92 × 40 × 5	Cold pressed	ČSN490113 ČSN490114	II : 111–144.75 ⊥ : 4.18–6.7
Sylvayanti et al. [58]	<i>Gigantochloa</i>	Indonesia	PF	460 × 25 × 25	Cold pressed	ASTM D143–14	II : 34.27
Wu et al. [59]	<i>Phyllostachys pubescens</i>	China	PF	370 × 20 × 15	Hot pressed	ASTM D143–14	II : 108.45 ⊥ : 7.62
Sewar et al. [62]	<i>Phyllostachys pubescens</i>	China	PF	375 × 25 × 25 63 × 50 × 50	Hot pressed	ASTM D143–14	II : 120.7 ⊥ : 7.7
Zheng et al. [64]	<i>Neosinocalamus affinis</i>	China	PF	370 × 20 × 15	Hot pressed	GB/T 1938–2009 ASTM D143–14	II : 250.2
Xu et al. [72]	<i>Phyllostachys pubescens</i>	China	PF	600 × 40 × 9	–	ASTM D143–14	II : 5.81–110.64 ⊥ : 0.73–6.68
Huang et al. [73]	<i>Phyllostachys</i>	China	–	453 × 25 × 5 57 × 50	–	ASTM D143–09	II : 118.4 ⊥ : 4.43
Yang et al. [74]	<i>Phyllostachys pubescens</i>	China	Epoxy	330 × 50 × 15	–	ASTM D143 ASTM C297	II : 108.7–138.9
Wang et al. [89]	<i>Phyllostachys pubescens</i>	China	–	370 × 20 × 15 150 × 30 × 20	–	GB/T 1938–2009 GB/T 14017–2009	II : 139.89–235.54 ⊥ : 11.41–17.82
Luo et al. [90]	<i>Phyllostachys pubescens</i>	China	PF	480 × 50 × 20	Hot pressed	LY/T 3194–2020	II : 141.92
Luo et al. [91]	<i>Phyllostachys pubescens</i>	China	PF	480 × 70 × 20	Hot pressed	LY/T 3194–2020	⊥ : 8.5

Table 4: Literature on shear properties

Study	Species	Origin	Glue	Shear		Standard	Strength (MPa)
				Size (mm)	Method		
Li et al. [20]	<i>Phyllostachys pubescens</i>	China	–	–	Hot pressed	GB/T 1937–2009	II : 52.41
Li et al. [48]	<i>Phyllostachys pubescens</i>	China	PF	63 × 50 × 50	–	–	II : 26.7
Sharma et al. [50]	<i>Phyllostachys pubescens</i>	China	PF	50 × 50 × 50	–	ASTM D143–09 BS 373 BS EN 408	II : 15
Kumar et al. [55]	<i>Phyllostachys pubescens</i>	China	PF	50 × 40 × 20	Cold pressed	ČSN490118	II : 11.89–17
Sylvayanti et al. [58]	<i>Gigantochloa</i>	Indonesia	PF	63 × 50 × 30	Cold pressed	ASTM D143–14	II : 11.15
Wu et al. [59]	<i>Phyllostachys pubescens</i>	China	PF	40 × 35 × 20	Hot pressed	ASTM D143–14	II : 20.89 ⊥ : 22.91–31.68
Sewar et al. [62]	<i>Phyllostachys pubescens</i>	China	PF	76 × 56 × 5	Hot pressed	ASTM D7080	II : 24 ⊥ : 37.1
Hu et al. [63]	<i>Phyllostachys pubescens</i>	China	PF	120 × 40 × 20	Hot pressed	GB/T 30364	–
Zheng et al. [64]	<i>Neosinocalamus affinis</i>	China	PF	40 × 35 × 20	Hot pressed	GB/T 1938–2009 ASTM D143–14	II : 29.6

(Continued)

Table 4 (continued)

Study	Species	Origin	Glue	Shear			
				Size (mm)	Method	Standard	Strength (MPa)
Rao et al. [68]	<i>Phyllostachys pubescens</i>	China	PF	78 × 40 × 13	Hot pressed	GB/T 30364–2013 GB/T 17657–2013 GB/T 20241–2006	⊥: 19.21
Shangguan et al. [71]	<i>Neosinocalamus affinis</i>	China	PF	40 × 35 × 20	Hot pressed	GB 1937–2009 ASTM D143–2009	–
Huang et al. [73]	<i>Phyllostachys</i>	China	–	76 × 56	–	ASTM D143–09 ASTM D7078	∥: 8.21 ⊥: 23.44
Yang et al. [74]	<i>Phyllostachys pubescens</i>	China	Epoxy	120 × 60 × 15/17	–	ASTM D143 ASTM-D7078	⊥: 33.8–46.1
Rao et al. [76]	<i>Phyllostachys pubescens</i>	China	PF	52 × 40 × 8.6	–	GB/T 17657–2013 GB/T 20241–2006	⊥: 16.3–21.7
Sun et al. [77]	<i>Phyllostachys pubescens</i>	China	PF	60 × 20 × 10	Hot pressed	GB/T 30364–2013 GB17657–2013	–
Yu et al. [84]	<i>Neosinocalamus affinis</i>	China	PF	90 × 40 × 18	Hot pressed	ASTM D-1037 ASTM D2344	–

It can be seen from the above four tables that China is the main producer of BS. *Neosinocalamus affinis* and *Phyllostachys pubescens* are the most commonly used BS raw materials. According to references [46–48,92,93], the properties of BS made from two kinds of raw bamboo are enhanced on the basis of raw materials, but the properties of the two kinds of BS are different from each other. In general, the tensile and compressive properties of BS with *Neosinocalamus affinis* as raw material are better than those of *Phyllostachys pubescens*. PF and epoxy are mostly used as adhesives, and the standards referenced in the test are mainly the standards related to wood in China and America. In the four mechanical property tests, the size of compression and bending test specimens changes greatly.

3 Reviews on Mechanical Properties

According to the review of BS mechanical properties, the commonly used test methods for BS mechanical properties test are shown in Fig. 3. The yellow part represents the specimen, and the red arrow represents the force and its direction.

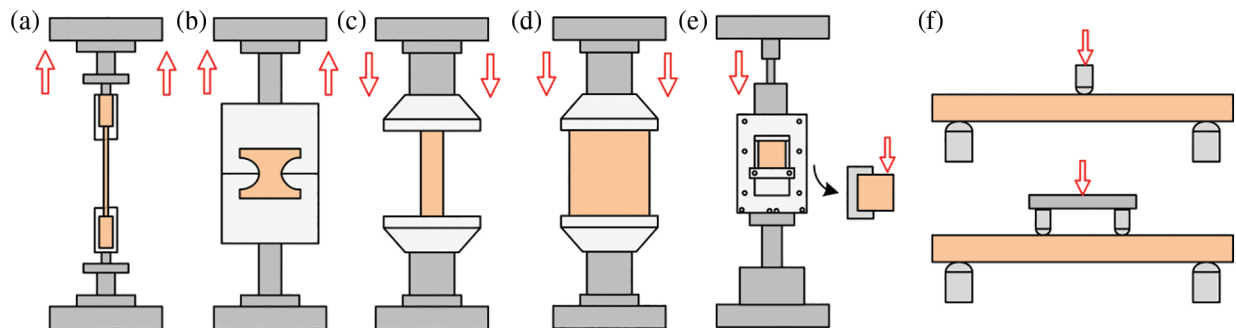


Figure 3: Schematic diagram of mechanical test: (a) tension parallel to grain, (b) tension perpendicular to grain, (c) compression parallel to grain, (d) compression perpendicular to grain, (e) shear parallel to grain, (f) three-point and four-point bending

3.1 Compression

In the compressive test of BS, the failure modes of compression parallel and perpendicular to grain can be divided into strength failure and buckling failure, and the buckling failure mostly occurs in the specimens with large slenderness ratio [69]. The compressive strength failure along the grain direction can be divided into three failure modes: buckling failure, shear failure and splitting failure [49,60], which are mainly due to the yield of fibers and the bond failure between fibers during loading. Oblique shear failure mainly occurs during compression perpendicular to grain [69,73], and the failure is mainly due to the bond failure between fibers (Fig. 4).



Figure 4: Compression failure forms: (a) parallel to grain. Adapted with permission from [60], Copyright © 2020, Elsevier B. V; (b) perpendicular to grain. Adapted with permission from [69], Copyright © 2019, Tech Science Press

The BS made by hot pressing at 140°C reduces the color deepening while maintaining its high durability, and its compressive strength is higher than that of ordinary BS [48,62]. The BS made of wide-bundle bamboo strips (WBS) has higher utilization rate of bamboo than the traditional BS, and the cracks caused by the fiberization of wide-bundle bamboo strips form a mechanical interlocking network filled with resin after resin filling and curing, which enhances the mechanical properties of WBS, so the compressive performance of WBS is better than that of traditional BS [63].

In the case of sufficient research on the mechanical properties of BS, it is of great significance to obtain the strength design value through reliability analysis. According to the damage characteristics of material test, the reliability index of design strength during compression is 3.2, the loading duration and reliability index are negatively correlated with the strength design value [64].

Shangguan et al. [71] studied the compression of BS made from different fiber orientations, and explored the influence of fiber orientation on the compressive properties and failure forms of BS. The results show that as the fiber orientation tends to be horizontal, the compressive strength of BS decreases, and the fiber buckling is less and less, mostly glue cracking and splitting between fibers. The longitudinal, tangential and radial compression tests show that the failure of the specimens caused by three loading directions is strength failure, and there are main cracks along the diagonal, the load-displacement curves in three grain directions include three stages of elasticity, yield and failure [51,56]. In the microscopic observation of the failure mode, it is shown that the fiber fracture of the longitudinal compression specimen is ductile, and the fiber fracture of the tangential and radial compression specimens is brittle, which is the reason why the deformation and strength of the longitudinal compression are greater than those of the tangential and radial compression [56]. However, when the temperature rises to a certain extent, due to the degradation of the resin, the ductile failure of BS parallel to grain will be transformed into brittleness, and the crushing failure occurs in the transverse direction [57]

In the composite test of BS and steel tube, it is found that the steel tube significantly increases the compressive strength and axial strain of BS, and restrains the lateral deformation of BS well. The thickness of steel tube has a great influence on the compressive strength and ultimate strain of BS [65]. The results of the composite test of glass fiber (GF) and BS show that the compressive strength of BS can be slightly increased when the GF layer is thicker, and GF significantly improves the fire resistance of BS [66].

The compressive properties of BS are affected by density [55]. As can be seen from Fig. 5, with the increase of the density of BS, the compressive strength and compressive modulus also increase, but the increase ratio decreases. The high density of BS makes its compressive properties higher than timber [58,59]. The effect of resin content on the compressive properties of BS was studied. Some experiments showed that the effect was not significant, but some experiments showed that the effect was significant [61,76,77].

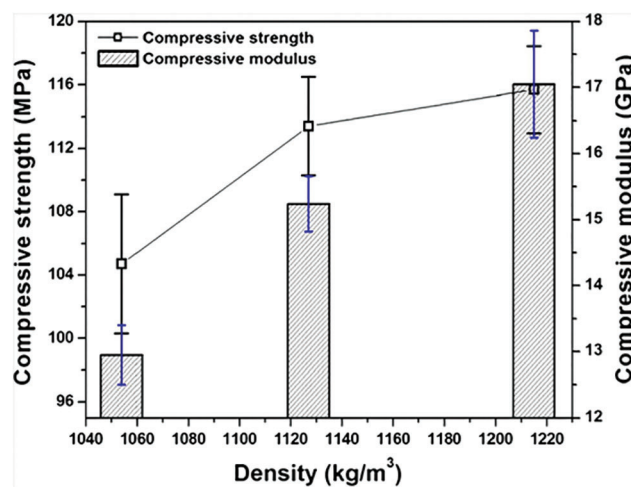


Figure 5: Compressive properties of different densities. Adapted with permission from [55], Copyright © 2016, Elsevier B. V

The creep study of BS showed that when BS is continuously compressed, the creep deformation develops stably when the stress level is low, the direct buckling failure when the stress level is high, and the deformation increases nonlinearly. In addition, the studies show that burgers model can better fit the creep curve of BS [52–54,67].

Burgers model is a quaternion model formed by Maxwell model and Kelvin model in series connection. Burgers model (Fig. 6) consists of three parts: instantaneous elastic deformation, delayed elastic deformation and viscous flow. The elastic element with elastic modulus E_1 in Maxwell model is used to simulate the instantaneous elastic deformation, the delayed elastic deformation is simulated by Kelvin model, and the viscous flow is simulated by the element with viscosity η_1 related to Maxwell model [54].

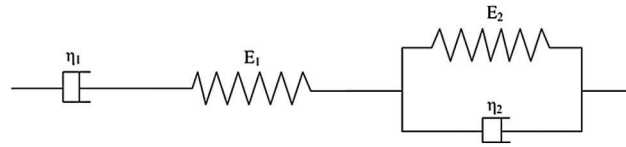


Figure 6: Burgers model

The equation of Burgers model is composed of the sum of Maxwell model and Kelvin model strain equation. The strain equations of Maxwell model and Kelvin model are both obtained on the basis of elastic equation and viscous equation.

Elastic equation:

$$\varepsilon = \frac{\sigma}{E} \quad (1)$$

Viscous equation:

$$\varepsilon = \frac{\sigma_0}{\eta} t \quad (2)$$

Maxwell model creep equation:

$$\varepsilon = \frac{\sigma_0}{E_1} \left(1 + \frac{E_1}{\eta_1} t \right) \quad (3)$$

Kelvin model creep equation:

$$\varepsilon = \frac{\sigma_0}{E_2} \left[1 - \exp\left(-\frac{E_2}{\eta_2} t\right) \right] \quad (4)$$

Burgers model creep equation:

$$\varepsilon(t) = \frac{\sigma_0}{E_1} + \frac{\sigma_0}{\eta_1} t + \frac{\sigma_0}{E_2} \left[1 - \exp\left(-\frac{E_2}{\eta_2} t\right) \right] \quad (5)$$

In order to quantitatively describe the flexibility and recovery performance of BS short columns, Wei et al. [70] studied the compression behavior of BS under cyclic load. It is found that the failure forms of BS short columns under cyclic load are the same as those under uniaxial compression, which are buckling, shear and splitting failure respectively, and the cyclic stress-strain model is established to predict.

Through the summary of the research on the compressive mechanical properties of BS, it is found that there is an obvious nonlinear section in the stress-strain curve of BS whether it is compressive parallel to grain or perpendicular to grain (as shown in Fig. 7), and the treatment methods for this nonlinear section are different [48,59,69,73]. In Table 5, the compression constitutive model of BS is summarized.

Table 6 shows the comparison of compressive properties between BS and other bamboo or wood materials.

Table 5: Compression constitutive model

Direction	Model	Formula	Coefficient
Perpendicular to grain	Quadratic function model [69]	$\sigma' = \begin{cases} E'_c \varepsilon' & 0 \leq \varepsilon' \leq \varepsilon'_{cy} \\ f'_{c0} \left[1 + a' \left(1 - \frac{\varepsilon'}{\varepsilon'_{c0}} \right)^2 \right] & \varepsilon'_{cy} \leq \varepsilon' \leq \varepsilon'_{c0} \end{cases}$	$a' = \frac{k'n' - 1}{(n' - 1)^2}, n' = \frac{\varepsilon'_{cy}}{\varepsilon'_{c0}}, k' = \frac{E'_c}{E'_p}$
	Exponential function model [73]	$\sigma' = \begin{cases} E'_c \varepsilon' & 0 \leq \varepsilon' \leq \varepsilon'_{cy} \\ \kappa \varepsilon'^n & \varepsilon'_{cy} \leq \varepsilon' \leq \varepsilon'_{c0} \end{cases}$	$n = \frac{\ln(f'_{cy}/f'_{c0})}{\ln(\varepsilon'_{cy}/\varepsilon'_{c0})}$ $\kappa = f'_{cy}/(\varepsilon'_{cy})^n$
Parallel to grain	Three-linear model [48]	$\sigma = \begin{cases} E_{cs} \varepsilon & (0 \leq \varepsilon \leq \varepsilon_{cy}) \\ f_{c0} \left[1 - a \left(1 - \frac{\varepsilon}{\varepsilon_{c0}} \right) \right] & (\varepsilon_{cy} \leq \varepsilon \leq \varepsilon_{c0}) \\ f_{c0} & (\varepsilon_{c0} \leq \varepsilon \leq \varepsilon_{cu}) \end{cases}$	$a = \frac{kn - 1}{n - 1}, n = \frac{\varepsilon_{cy}}{\varepsilon_{c0}}, k = \frac{E_{cs}}{E_p}$
	Quadratic function model [48,69]	$\sigma = \begin{cases} E_{cs} \varepsilon & (0 \leq \varepsilon \leq \varepsilon_{cy}) \\ f_{c0} \left[1 + a \left(1 - \frac{\varepsilon}{\varepsilon_{c0}} \right)^2 \right] & (\varepsilon_{cy} \leq \varepsilon \leq \varepsilon_{c0}) \\ f_{c0} & (\varepsilon_{c0} \leq \varepsilon \leq \varepsilon_{cu}) \end{cases}$	$a = \frac{kn - 1}{(n - 1)^2}, n = \frac{\varepsilon_{cy}}{\varepsilon_{c0}}, k = \frac{E_{cs}}{E_p}$
	The 2nd order polynomial [73]	$\sigma = \begin{cases} E_{cs} \varepsilon & (0 \leq \varepsilon \leq \varepsilon_{cy}) \\ \lambda_1 \varepsilon^2 + \lambda_2 \varepsilon + \lambda_3 & (\varepsilon_{cy} \leq \varepsilon \leq \varepsilon_{c0}) \\ \beta_1 \varepsilon^2 + \beta_2 \varepsilon + \beta_3 & (\varepsilon_{c0} \leq \varepsilon \leq \varepsilon_{cu}) \end{cases}$	$\lambda_1 = \frac{f_{cy} - f_{c0}}{(\varepsilon_{cy} - \varepsilon_{c0})^2}$ $\lambda_2 = \frac{2\varepsilon_{c0}(f_{c0} - f_{cy})}{(\varepsilon_{c0} - \varepsilon_{cy})^2}$ $\lambda_3 = \frac{(\varepsilon_{cy})^2 f_{c0} - 2\varepsilon_{cy}\varepsilon_{c0}f_{c0} + (\varepsilon_{c0})^2 f_{cy}}{(\varepsilon_{c0} - \varepsilon_{cy})^2} \quad \beta_1 = \frac{f_{c0} - f_{cu}}{(\varepsilon_{c0} - \varepsilon_{cu})^2}$ $\beta_2 = \frac{2\varepsilon_{cu}(f_{cu} - f_{c0})}{(\varepsilon_{cu} - \varepsilon_{c0})^2}$ $\beta_3 = \frac{(\varepsilon_{c0})^2 f_{cu} - 2\varepsilon_{c0}\varepsilon_{cu}f_{cu} + (\varepsilon_{cu})^2 f_{c0}}{(\varepsilon_{cu} - \varepsilon_{c0})^2}$
	Compound function model [59]	$\sigma = \begin{cases} E_{cs} \varepsilon & (0 \leq \varepsilon \leq \varepsilon_{cy}) \\ f_{c0} \left[1 + a \left(1 - \frac{\varepsilon}{\varepsilon_{c0}} \right)^2 \right] & (\varepsilon_{cy} \leq \varepsilon \leq \varepsilon_{c0}) \\ f_{c0} + 0.16E_p(\varepsilon - \varepsilon_{c0}) & (\varepsilon_{c0} \leq \varepsilon \leq \varepsilon_{cu}) \end{cases}$	$a = \frac{kn - 1}{(n - 1)^2}, n = \frac{\varepsilon_{cy}}{\varepsilon_{c0}}, k = \frac{E_{cs}}{E_p}$
	Cubic function model [48]	$\sigma = \begin{cases} E_{cs} \varepsilon & (0 \leq \varepsilon \leq \varepsilon_{cy}) \\ f_{c0} \left[a_0 + a_1 \left(\frac{\varepsilon}{\varepsilon_{c0}} \right) + a_2 \left(\frac{\varepsilon}{\varepsilon_{c0}} \right)^2 + a_3 \left(\frac{\varepsilon}{\varepsilon_{c0}} \right)^3 \right] & (\varepsilon_{cy} \leq \varepsilon \leq \varepsilon_{c0}) \\ f_{c0} & (\varepsilon_{c0} \leq \varepsilon \leq \varepsilon_{cu}) \end{cases}$	$a_0 = 1 + \frac{2n(kn - 1) + (1 - n)}{(n - 1)^3}$ $a_1 = \frac{2n(3 - 2kn) - k(n + 1)}{(n - 1)^3}$ $a_2 = \frac{(2kn - 3)(n + 1) + 2k}{(n - 1)^3}$ $a_3 = \frac{2 - k(n + 1)}{(n - 1)^3}$ $n = \frac{\varepsilon_{cy}}{\varepsilon_{c0}}, m = \frac{\sigma_{cy}}{f_{c0}}, k = \frac{E_{cs}}{E_p}$

Note: σ is the stress value of BS under compression parallel to grain; E_{cs} is the modulus of elasticity for BS under compression parallel to grain; E_p is the secant modulus for peak point (f_{c0}, ε_{c0}); ε is the strain value of BS; ε_{cy} is the strain for the yield point; ε_{c0} is the compression peak strain value; f_{c0} is the compression peak stress value; ε_{cu} is the ultimate compression strain value; f_{cu} is the ultimate compression stress value; σ' is the stress value of BS under compression perpendicular to grain; E'_c is the modulus of elasticity for BS under compression perpendicular to grain; E'_p is the secant modulus for peak point; ε' is the strain value of BS; ε'_{cy} is the strain for the yield point; f'_{cy} is the stress for the yield point; ε'_{c0} is the compression peak strain value; f'_{c0} is the compression peak stress value.

In Table 6, LBL represents Laminated Bamboo Lumber which made from bamboo strips as manufacturing units and laminated with adhesive, WPC represents Wood-Plastic Composites.

It can be seen from the table that the compressive strength and MOE of BS are significantly higher than those of other materials. The change of compressive strength of BS can be attributed to the different types of bamboo used in the production of BS and the different density of BS itself.

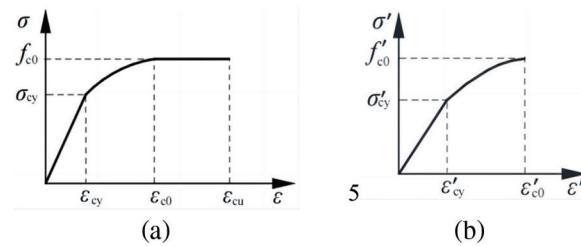


Figure 7: Compressive stress-strain curves of BS: (a) parallel to grain; (b) perpendicular to grain. Adapted with permission from [69], Copyright © 2019, Tech Science Press

Table 6: Comparison of compressive properties

Material	Species	Size (mm)	Compression (MPa)	Compression ⊥ (MPa)	MOE (MPa)	MOE ⊥ (MPa)
BS [50,69]	Phyllostachys pubescens	60 × 20 × 20 50 × 50 × 50 100 to 200 × 50 × 50	86–102.1	37–54.4	13994–14222	4285–4383
LBL [94,95]	Phyllostachys pubescens	200 × 50 × 50 300 × 20 × 20 60 × 20 × 20	37.58–64.7	–	5875.7–13379	–
Glulam [96]	–	–	24–31	2.7–3.6	8600	–
WPC [97]	Pine	60 × 20 × 20	28.1	25.4	3700	1980
Plywood [98]	–	–	20.7–34.5	–	–	–
Douglas-fir [99]	–	–	49.9	5.5	–	–

3.2 Bending

The three-point bending and four-point bending test methods are used for the bending specimens of BS. The bending strength parallel to grain of the bending small specimens of BS without special treatment is usually between 100–150 mpa, and the failure mode is that the fiber in the tensile area is broken [17,48,58]. The bending properties MOR and MOE of BS increase with density [63].

Taking natural bamboo as the comparison object, it is found that the failure mode of BS shows obvious brittleness, and the bending failure is the result of the joint action of tensile, shear and compressive stress [88]. According to the analysis of the bending load displacement curve of BS, its bending damage is between toughness and brittleness [62,64]. Compared with natural bamboo, the deformability of BS is reduced and the brittleness is increased, which is due to the compression of the cavities of the vessel and parenchymal cells that absorb energy in the manufacturing process [88].

When the length of the specimen is changed, it is found that the bending strength does not change significantly with the increase of the length, while the bending elastic modulus increases with the increase of the length [85].

It was found in the study of the effect of resin content on the bending properties of BS, the change of resin content does not change its damage form [68]. The MOR of BS increases slightly with the increase of resin content, but decreases when the content exceeds 20%, which has a negative impact on the bending properties of BS, and the bending bearing capacity also reaches the maximum at 20%. However, some studies have shown that when the resin content of BS is 15%, its MOR and MOE reach the maximum [61]. The flexural strength increases with the increase of resin content and density, while the flexural modulus is less affected by resin content and increases with the increase of density [84].

Zou et al. [82] studied the effect of moisture content. Although the bending strength of BS showed a downward trend with the increase of moisture content, the fiber fracture degree at failure gradually decreased, and the failure mode showed certain plasticity.

The study on the bending performance of BS with different fiber orientation shows that the bending strength and stiffness decrease with the increase of the included angle between bamboo fiber and neutral axis. Moreover, the failure mode gradually changes from the ductile failure of fiber breaking to the shear brittle failure of bonding interface, and the crack extends rapidly along the interface, resulting in the brittle fracture of the specimen [80]. At the same time, the fiber orientation also greatly affects the impact bending property [86,87].

In engineering, in order to facilitate the transportation of wires and the assembly of structures, it is usually necessary to drill holes. Zhao et al. [81] drilled holes in different positions and sizes of bending small specimens of BS to study and compare their bending properties. The results show that drilling reduces the bearing capacity and bending properties of the specimen, and the larger the hole diameter is, the more obvious the reduction is. At the same time, due to drilling, there are two basic failure modes of bending small specimens-shear failure along the fiber direction and bottom fracture failure caused by bending moment.

FRP is a lightweight and high-strength material with excellent reinforcing properties. The mechanical properties of the material reinforced with FRP are generally significantly improved [100–102]. In order to solve the problem of low bending strength and stiffness of BS, Wu et al. [83] studied the CFRP-BS composite beam. It is found that the CFRP sheet effectively improves the bending modulus and static bending strength of the composite beam, and the failure mode is no longer the fracture failure of the bottom fiber, but the bond failure between CFRP and BS. However, the research of Liu et al. [78] shows that the failure modes of CFRP-BS composite beams are divided into four types under different conditions: CFRP ‘flowering’ fracture failure, gradual peeling failure of the adhesive layer, instantaneous peeling failure of the adhesive layer and fracture failure of BS.

The BS beam can obtain greater bearing capacity and deflection under the same shear span ratio by means of bamboo pin reinforcement, and increasing the spacing of bamboo pins can improve the bearing capacity and stiffness of the reinforced beam. At the same time, as the load continues to increase, the failure of the epoxy resin adhesive layer in the hole leads to an increase in slip, which generally increases linearly. After parallel-to-grain shear failure, the load-slip increases nonlinearly and the slip increases significantly [79].

Table 7 shows the comparison of mechanical properties of BS with other bamboo and wood materials under bending conditions.

In Table 7, LLBC represents Layered Laminate Bamboo Composite which made from thinner and shorter bamboo strips than LBL by laminating with more adhesive, LVL represents Laminated Veneer Lumber which made from wood and adhesive by hot pressing.

It can be seen that the bending strength of BS can be comparable with other bamboo-based materials (such as LBL and LLBC) and wood (such as Douglas fir). At the same time, the bending strength of BS is significantly better than LVL, Glulam, WPC and plywood. The change of bending strength of BS may be related to density, adhesive and bamboo species.

3.3 Tension

When studying the tensile properties of BS, the specimen is usually prepared into bone shape. During the tensile test parallel to grain, the failure form of the tensile specimen is that part of the fiber is first broken under the load, and then the crack develops rapidly, forming a fracture surface in a short time, and finally the specimen is completely destroyed. The fracture surface is irregular in most cases. Only when the fiber

distribution of the sample is uniform, the fracture surface is flat and almost perpendicular to the fiber [48,58,59,62,64,73].

Table 7: Comparison of bending properties

Material	Species	Size (mm)	Bending (MPa)	MOE (MPa)
BS [20,50]	Phyllostachys pubescens	800 × 40 × 40	81.6–125.44	11341–16310
LBL [94]	Phyllostachys pubescens	760 × 50 × 50	98–126.3	7955–11190
LLBC [98,103]	Dendrocalamus strictus	250 × 16 × 10	100.8	12420
LVL [99]	Douglas-fir	–	54.2–71.7	15400–19300
Glulam [104]	Douglas-fir	–	48.74	15370
WPC [97]	Pine	67 × 10 × 4	26.1	4100
Plywood [99]	Redwood	–	33.72–42.61	6960–8550
Douglas-fir [99]	–	–	85	13400

The tensile strength parallel to grain of BS is generally between 100–250 MPa due to the type of original bamboo and manufacturing technology [21,46,48]. However, it should be noted that the tensile strength perpendicular to grain of BS is about 40 times lower than that parallel to grain, and the location of cracks changes during failure. Cracks are produced through the bamboo itself rather than simply through the adhesive [20,50].

The stress-strain curve of tension parallel to grain increases linearly and has a certain discreteness. But the stress-strain curve of transverse tension has a nonlinear stage, and it has greater discreteness than that of longitudinal tension (as shown in Fig. 8) [48].

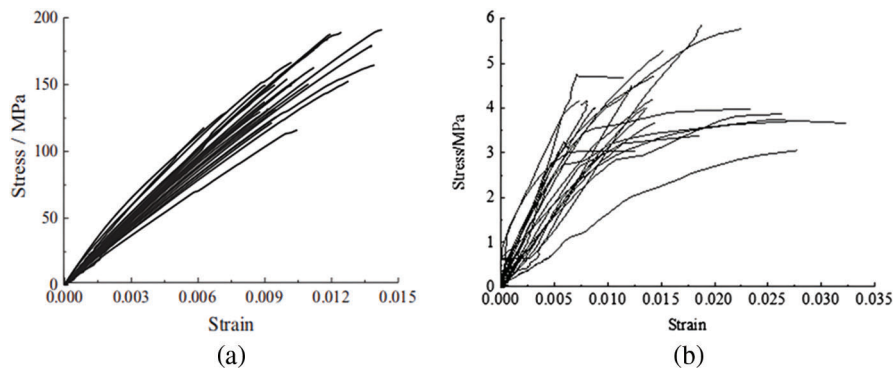


Figure 8: Tensile stress-strain curves: (a) parallel to grain, (b) perpendicular to grain. Adapted with permission from [48], Copyright © 2020, Tech Science Press

It is worth noting that the tensile failure parallel to grain of carbonized BS shows brittleness, and the tensile strength and elastic modulus parallel to grain of carbonized BS are less than those of non-carbonized one [47]. The tensile creep behavior of BS shows brittle fracture under high load (60% ultimate strength), while at low load (lower than 40% ultimate strength), the creep deformation of BS develops rapidly in the early stage and remains stable in the middle and late stage. The load level has a significant impact on the overall creep deformation and the proportion of creep deformation [53].

BS with different densities were tested according to the standard ČSN 490113 and ČSN 490114 carries out tensile tests parallel and perpendicular to grain (as shown in Fig. 9). The results show that the tensile strength increases with the increase of density, and the tensile strength parallel to grain is always 20–30 times that of perpendicular to grain [55].

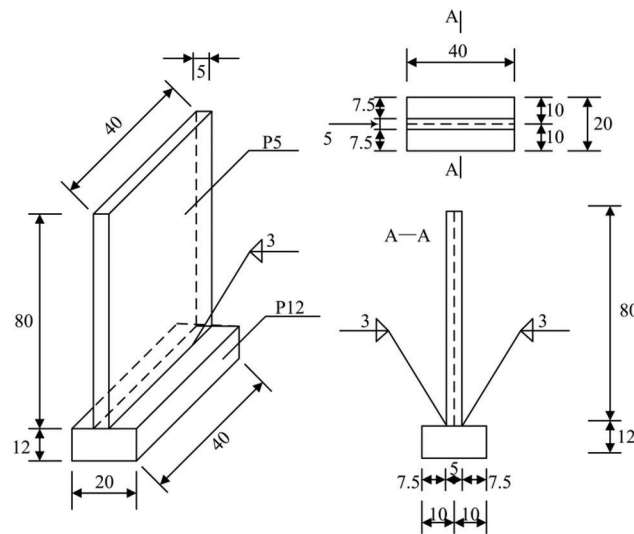


Figure 9: Perpendicular tensile test. Adapted with permission from [55], Copyright © 2016, Elsevier B. V

The long-term performance of the material is related to its own application value, so the long-term tensile behavior of BS is worth studying. In the long-term tensile test of BS, it is found that the load duration in the transverse direction of BS is less than that in the longitudinal direction. The relationship between the stress ratio and the failure time in the transverse direction is close to the Madison curve, while the longitudinal direction is concave trend curve. The empirical Findley model can well fit the absolute creep strain-time curves in both directions [90,91].

Wang et al. [89] studied the tensile properties of BS under different strain rates, and conducted impact tensile test with split Hopkinson tensile bar. It is found that the ultimate tensile strength increases with the increase of strain rate; In addition, no matter static tensile test or impact tensile test, the failure forms of BS are I-shaped fracture and Z-shaped fracture when tension parallel to grain, and flat fracture when tension perpendicular to grain. At the same time, the fracture surface of the specimen was observed by electron microscope to study its failure mechanism. It is found that for the tensile failure parallel to grain, the failure process can be considered as three processes: matrix fracture, interface fracture and fiber fracture. For tensile failure perpendicular to grain, the damage is mainly caused by interface fracture. The pore on the cemented surface is the root of the initial crack. Because the fiber is not affected by force, the crack expands along the interface and finally the specimen breaks (Fig. 10 is the Scanning Electron Microscope (SEM) observation).

According to the research of Xu et al. [72], when the temperature is between 20°C–180°C, the tensile strength and modulus of BS decrease with the increase of temperature, but when the temperature rises to 200°C, the tensile strength and modulus parallel to grain of BS first rise and then continue to decline, while the tensile strength and modulus perpendicular to grain of BS decrease to 0 when the temperature rises to 200°C and above. Moreover, the tensile failure forms parallel to grain of BS are divided into I-shape and Z-shape, but the I-shaped fracture mainly occurs in the tensile fracture at the temperature above 180°C, while the failure form of tension perpendicular to grain is I-shaped failure at any temperature.

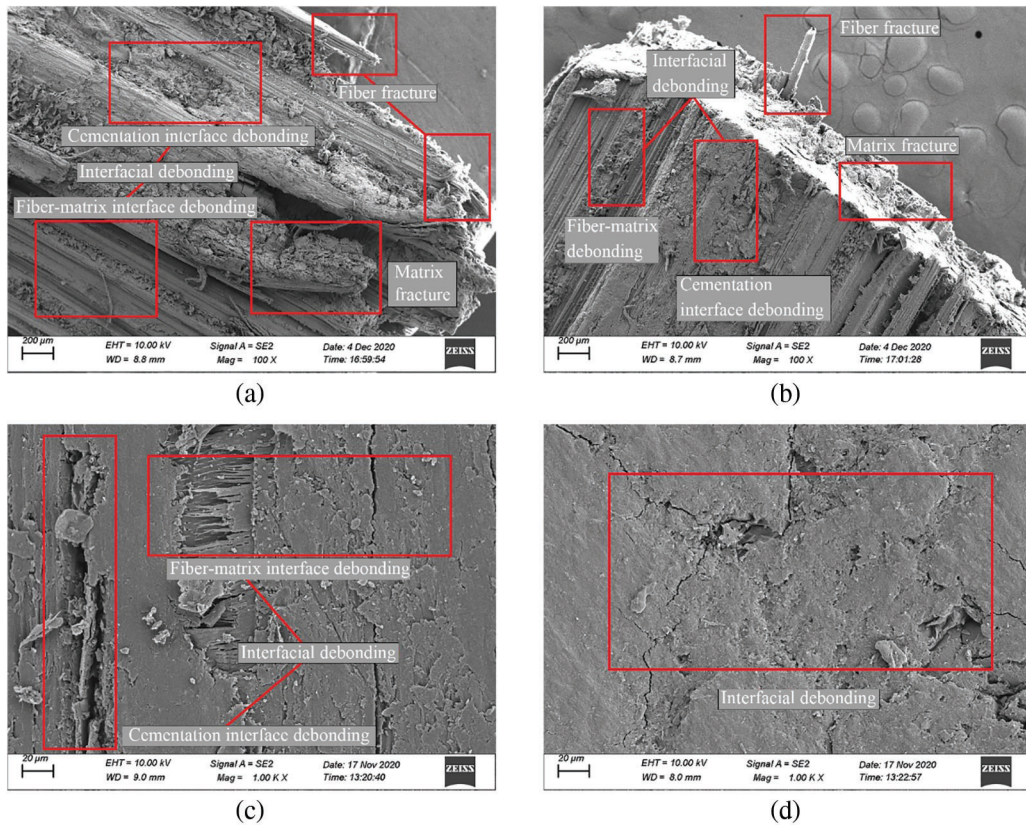


Figure 10: Typical SEM observation of (a) quasi-static longitudinal, (b) impact longitudinal, (c) quasi-static transverse and (d) impact transverse BS samples. Adapted with permission from [89], Copyright © 2021, Elsevier B. V

Table 8 shows the comparison of mechanical properties between BS and other bamboo and wood materials under tensile conditions.

Table 8: Comparison of tensile properties

Material	Species	Size/mm	Tension \parallel (MPa)	Tension \perp (MPa)	MOE \parallel (MPa)	MOE \perp (MPa)
BS [50,73]	Phyllostachys pubescens	460 × 25 × 25 62 × 50 × 50 250 × 19 × 7 to 8 453 × 25 × 5 57 × 50	118.4–138	3–4.43	10296–13680	3066
LBL [50,94]	Phyllostachys pubescens	460 × 25 × 25 62 × 50 × 50 453 × 50 × 25	90–125.9	2	9663–12476	–
LLBC [98,103]	Dendrocalamus strictus	250 × 16 × 10 200 × 15 × 1.5	187.3	–	14900	–
LVL [94,105]	Douglas-fir	–	88.5	0.83	13790	–
Glulam [96]	–	–	16.5–26	0.4–0.6	9400–11900	390–490
WPC [97]	Pine	–	11.6	5.3	3000	1500
Plywood [98]	–	–	10.3–27.6	–	–	–
Douglas-fir [99]	–	–	107.6	2.3	11.6–14.8	–

It can be seen that the tensile strength parallel to grain and MOE of BS are similar to LBL, higher than other materials, but lower than LLBC. In terms of tensile strength perpendicular to grain, the tensile strength of BS can be comparable to that of WPC and Douglas fir, surpassing that of wood-based materials such as LVL and Glulam.

3.4 Shear

It can be seen from relevant researches [50,55,58,64] that the failure surface of BS is rough during the shear failure parallel to the grain, the shear strength parallel to the grain is between 10–20 Mpa, and the shear strength increases with the increase of the density of BS [63].

Yu et al. [84] studied the shear strength of BS with different resin content and density. The results showed that the shear strength increased with the increase of resin content and density. However, according to literature [63,88,89], the test results show that increasing the resin content has no obvious effect on the shear strength of BS.

In the shear test of BS in different fiber directions with reference to ASTM D7078, it is found that the failure modes of shear parallel to grain and in transverse-to-grain-plane are almost the same, both of which are a crack, tear the specimen into two halves symmetrically, and the stress-strain curve is approximately linear. In transverse shear, the shear action is basically caused by the tension of the fiber in the notch range. Cracks along the fiber direction can be observed, but the specimen is still a whole, and the stress-strain curve is nonlinear [62,73]. The failure modes and stress-strain curves are shown in Fig. 11.

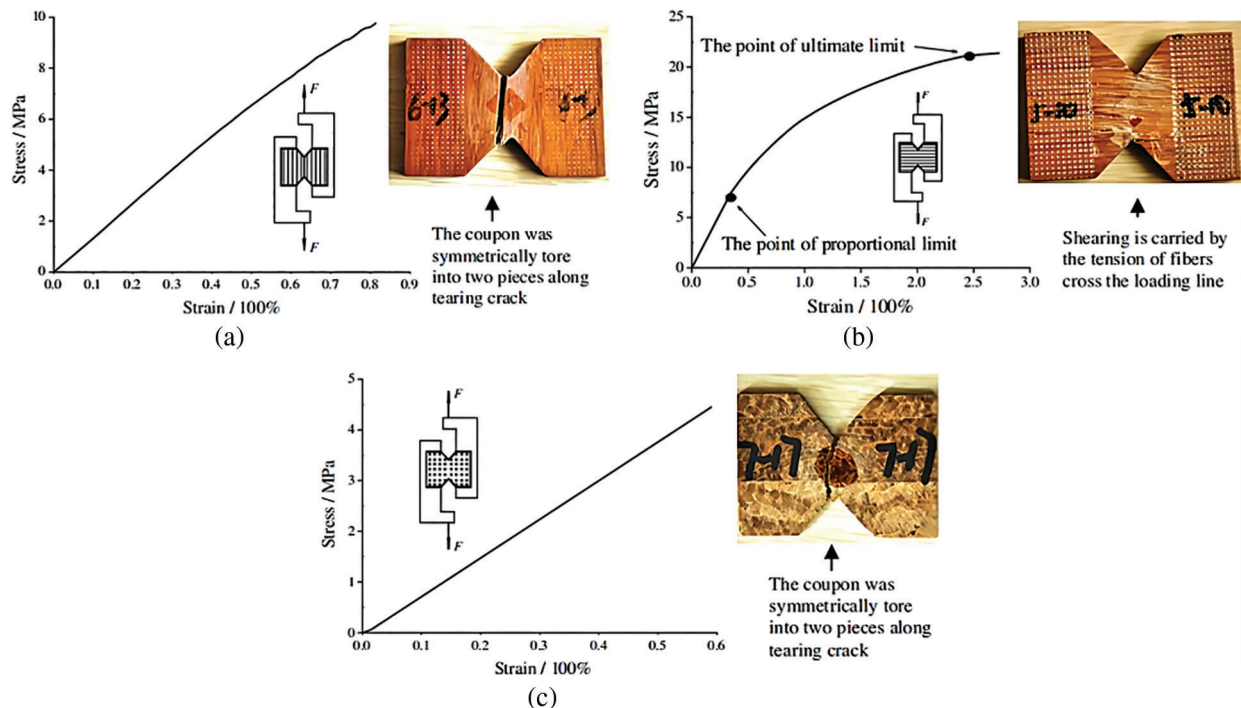


Figure 11: Stress–strain relationship and failure mode of shear: (a) parallel to grain, (b) perpendicular to grain, (c) in transverse-to-grain-plane. Adapted with permission from [73], Copyright © 2014, Elsevier B. V

Yang et al. [74] compared the shear properties perpendicular to grain of BFRP-BS and ordinary BS. It is found that for ordinary BS cracks appear along the fiber direction at the notch and develop longitudinally, then the longitudinal cracks change into transverse cracks, and finally fail with the expansion of cracks. The failure of BFRP-BS is caused by the fracture of BFRP material in the notch, and BFRP can enhance the shear strength of BS to a certain extent. The failure modes are shown in Fig. 12.

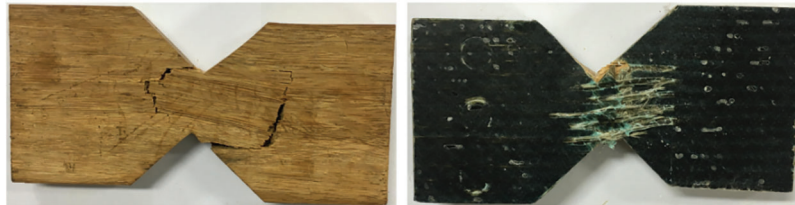


Figure 12: Shear strength of BS with different resin content and density. Adapted with permission from [74], Copyright © 2020, Elsevier B. V

Table 9 shows the comparison of mechanical properties between BS and other bamboo and wood materials under shear conditions.

Table 9: Comparison of tensile properties

Material	Species	Size (mm)	Shear II (MPa)	Shear \perp (MPa)
BS [50,55,73]	Phyllostachys pubescens	50 × 50 × 50 50 × 40 × 20 76 × 56	8.21–17	23.44
LBL [103,106]	Phyllostachys pubescens	62 × 50 × 50 50 × 50 × 17	7.15–17.5	–
Glulam [107]	–	50 × 50 × 40	16.9	17.5
LVL [108]	lodgepole pine	64 × 51 × 38 64 × 51 × 38	4.9–5.0	6.5–6.8
WPC [97]	Pine	–	8.1	7.1
Douglas-fir [99]	–	–	7.8	–

It can be seen that compared with bamboo-based and wood-based materials such as LBL, LVL, WPC and Douglas fir, BS has similar or even higher shear strength, and the shear strength perpendicular to grain is better.

4 Discussion

BS and LBL are both popular engineering bamboo materials at present, with their own advantages and disadvantages. In terms of mechanical properties, BS is better than LBL. LBL is made by veneering bamboo slices. The existence of bamboo nodes will have different effects on the mechanical properties. For BS, because the bamboo strips have been fully defibered during the manufacture, there will be no problem of the influence of bamboo nodes [48,109]. However, BS is not widely used in buildings because it contains a large amount of glue and emits a strong odor. On the contrary, LBL has no such limitation because it contains less glue.

As a wood-like material made of bamboo, BS has better mechanical properties than many real Wood. Taking *Larix gmelini* and Sitka spruce as examples, BS is obviously better in the tensile and compressive strength parallel to grain and the bending strength [50,110,111]. However, whether the performance on the connecting joint can be comparable to that of wood remains to be further studied.

In terms of production, although the impact of BS on the environment is relatively low compared with traditional building materials, due to the use of adhesives and power equipment, the production of BS consumes more energy and produces more emissions compared with wood materials. Therefore, this requires the development of new cost-saving and low energy consumption manufacturing technologies, such as the improvement of adhesives and production equipment and the improvement of automation.

In terms of use, currently, BS is mainly used in the field of decoration and furniture, with few examples as building materials. This is related to its cost and its own peculiar smell, as well as the lack of a standard system as complete as wood. However, the lack of practical examples in turn leads to the difficulty in formulating the corresponding standard for BS. In this regard, the design, construction, management and other work processes of BS structure can be digitized and the structural stress analysis can be carried out through computer software.

5 Conclusion

This review summarizes the mechanical properties of BS under different loading modes. According to the literature review, the bamboo species used in the production of BS are mainly *Neosinocalamus affinis* and *Phyllostachys pubescens*. However, whether other bamboo species can be better applied to BS production remains to be studied.

According to the results of the literature review, the strength change of BS is affected by factors such as original bamboo type, growth position, resin content, treatment method, and density. Therefore, different production processes can be adopted according to different requirements, and BS can also be classified accordingly. The classification and standardization of BS will help practitioners around the world consider bamboo species, adhesive types, processing methods and strength to select the grade required for BS materials, so as to achieve the expected purpose.

Due to the gradual increase of research on the mechanical properties of BS, there is sufficient basis to form corresponding test standards for the mechanical properties of BS so as to promote the development and application of BS.

So far, there is not much construction and research on BS buildings. Therefore, the performance of BS in the overall building is not clear, which needs simulation research with the help of finite element or 3D-printing technology.

It may be an interesting direction in the future to apply artificial neural networks and topology optimization to the performance analysis and research of BS.

Acknowledgement: The writers gratefully acknowledge Yue Chen, Xing Guo, Bingyu Jan, Tingting Ling, Yukun Tian, Wei Xu, Dong Yang, Wenjing Zhou, Lincui Ge and others from the Nanjing Forestry University.

Funding Statement: This work was supported by the National Natural Science Foundation of China (Nos. 51878354 & 51308301); the Natural Science Foundation of Jiangsu Province (Nos. BK20181402 & BK20130978); 333 Talent High-Level Project of Jiangsu Province; Qinglan Project of Jiangsu Higher Education Institutions; and the Ministry of Housing and Urban-Rural Science Project of Jiangsu Province under Grant (No. 2021ZD10). Any research results expressed in this paper are those of the writer(s) and do not necessarily reflect the views of the foundations.

Author Contributions: Data collection: Xin Xue, Haitao Li, Rodolfo Lorenzo; analysis and interpretation of results: Xin Xue, Haitao Li; draft manuscript preparation: Xin Xue, Haitao Li.

Availability of Data and Materials: Data availability is not applicable to this article as no new data were created or analyzed in this study.

Conflicts of Interest: The authors declare that they have no conflicts of interest to report regarding the present study.

References

1. Zhou Y, Huang Y, Sayed U, Wang Z. Research on dynamic characteristics test of wooden floor structure for gymnasium. *Sustain Struct.* 2021;1(1):5. doi:10.54113/j.sust.2021.000005.
2. Ponzo FC, Antonio DC, Nicla L, Nigro D. Experimental estimation of energy dissipated by multistorey post-tensioned timber framed buildings with anti-seismic dissipative devices. *Sustain Struct.* 2021;1(2):7. doi:10.54113/j.sust.2021.000007.
3. Wang Z, Zhang X, Yao L, Zhang QM. Experimental study and numerical simulation on the macro and micro mechanical properties of bamboo. *J For Eng.* 2022;7(1):31–7. doi:10.13360/j.issn.2096-1359.202105031.
4. Xia T, Zhou Y, Zheng W, Dong L, Wang QZ, Zhao T. Failure mode and damage assessment of the midply-bamboo shear walls. *J For Eng.* 2022;7(3):53–9. doi:10.13360/j.issn.2096-1359.202109018.
5. Mergiauw T, Addissie D, Goedert J. Failure behavior and failure locations of *Oxytenanthera Abyssinica* bamboo culms under bending load. *Sustain Struct.* 2023;3(2):29. doi:10.54113/j.sust.2023.
6. Mei S, Zhao D, Meng X, Qi X, Gao Y. Experimental study on tensile properties of the arc outer green skin of bamboo. *J For Eng.* 2022;7(3):60–6. doi:10.13360/j.issn.2096-1359.202104033.
7. Wang J, Wu XY, Wang YJ, Zhao WY, Zhao Y, Zhao M, et al. Green, sustainable architectural bamboo with high light transmission and excellent electromagnetic shielding as a candidate for energy-saving buildings. *Nano-Micro Lett.* 2023;15(1):11. doi:10.1007/s40820-022-00982-7.
8. Shan B, Wang G, Lei PP, Li TY, Xiao Y, Qin SJ, et al. Experimental research on formaldehyde emission characteristics from glubam by climate chamber test. *Sustain Struct.* 2023;3(2):27. doi:10.54113/j.sust.2023.000027.
9. Das A, Mohanty K. Optimization of lignin extraction from bamboo by ultrasound-assisted organosolv pretreatment. *Bioresour Technol.* 2023;376:128884. doi:10.1016/j.biortech.2023.128884.
10. Liu KW, Jayaraman D, Shi YJ, Harries K, Yang J, Jin W, et al. Bamboo: a very sustainable construction material-2021 international online seminar summary report. *Sustain Struct.* 2022;2(1):15. doi:10.54113/j.sust.2022.000015.
11. Li R, Ekevad M, Guo X, Ding J, Cao P. Effect of pressure, feed rate, and abrasive mass flow rate on water jet cutting efficiency when cutting recombinant bamboo. *BioResources.* 2015;10:499–509. doi:10.15376/biores.10.1.499-509.
12. Yuan M, Feng X. Application of bamboo material in modern architecture. In: 5th International Conference on Civil Engineering and Transportation; 2015; Guangzhou, China, Atlantis Press. pp. 1905–11. 10.2991/iccet-15.2015.355.
13. Gong Z, Yuan SF, Zhang J, Wang HY, Li Q, Xu K. Research status and development trend of reconstituted bamboo lumber production equipment. *For Mach Woodworking Equip.* 2018;46:4–9. doi:10.13279/j.cnki.fmwe.2018.0093.
14. Wang X, Chen H, Hu M. Research status and development trend of recombinant bamboo. *Building Technol Develop.* 2018;45:4–5.
15. Yu W. Current status and future development of bamboo scrimber industry in China. *China Wood Ind.* 2019;17:1–4. doi:10.19455/j.mcgy.2012.01.005.
16. Banik N. Manufacturing of bamboo composite in the industrial aspect. *Mat Today: Proc.* 2020;26:2875–87. doi:10.1016/j.matpr.2020.02.596.

17. Zhou F. Studies on physical and mechanical properties of bamboo woods. *J Nanjing Technol College For Products*. 1981;5:1–32. doi:10.3969/j.jssn.1000-2006.1981.02.001.
18. Yu Y, Huang X, Yu W. High performance of bamboo-based fiber composites from long bamboo fiber bundles and phenolic resins. *J Appl Polym Sci*. 2014;131(12):40371. doi:10.1002/app.40371.
19. Awalluddin D, Ariffin MAM, Osman MH, Hussin MW, Ismail MA, Lee HS, et al. Mechanical properties of different bamboo species. *MATEC Web Conf*. 2017;138:1024. doi:10.1051/mateconf/201713801024.
20. Li X, Zhong Y, Ren H, Xiao G. Study on mechanical properties of recombinant bamboo produced by moso bamboo. *Wood Process Mach*. 2016;27:28–32. doi:10.13594/j.cnki.mcjgix.2016.04.008.
21. Gong YC, Zhang CQ, Zhao RJ, Xing XT, Ren HQ. Experimental study on tensile and compressive strength of bamboo scrimber. *BioResources*. 2016;11:7334–44. doi:10.15376/biores.11.3.7334-7344.
22. Huang MX, Zhang WB, Zhang XC, Li WZ, Yu WJ, Zhang H. Advances in bamboo softening and flattening technology. *J Bamboo Res*. 2015;34:31–6. doi:10.3969/j.jssn.1000-6567.2015.
23. Deng JC, Li HD, Wang G, Chen FM, Zhang WF. Effect of removing extent of bamboo green layer on physical and mechanical properties of laminated bamboo-bundle veneer lumber (BLVL). *Eur J Wood Wood Prod*. 2015;73:499–506. doi:10.1007/s00107-015-0897-x.
24. Chung MJ, Wang SY. Effects of peeling and steam-heating treatment on mechanical properties and dimensional stability of oriented *Phyllostachys makinoi* and *Phyllostachys pubescens* scrimber boards. *J Wood Sci*. 2018;64:625–34. doi:10.1007/s10086-018-1731-y.
25. Yu Y, Huang X, Yu W. A novel process to improve yield and mechanical performance of bamboo fiber reinforced composite via mechanical treatments. *Composites Part B: Eng*. 2014;56:48–53. doi:10.1016/j.compositesb.2013.08.007.
26. Zhang YM, Zhu RX, Yu YL, Yu WJ. Effects of the resin directional penetration by rolling technology on the drying process of bamboo bundles and bamboo scrimber properties. *J For Eng*. 2022;7(5):44–9. doi:10.13360/j.jssn.2096-1359.202108034.
27. Hou RG, Liu Y, Li XJ, Sun RH, Qiao JZ. Effects of heat treatment on physical-mechanical properties of reconstituted bamboo lumber (RBL). *J Central South Univ Technol*. 2013;33:101–4. doi:10.14067/j.cnki.1673-923x.2013.02.023 (In Chinese).
28. Cheng L, Wang X, Yu Y. Effect of glue immersion parameters on performance of reconstituted *Dendrocalamopsis oldhami* lumber. *China Wood Ind*. 2009;23:16–9. doi:10.19455/j.mcgy.2009.03.005 (In Chinese).
29. Wang Y, Li XJ, Lv JX, Xu K, Wu YQ. Optimization adhesive impregnation conditions of bamboo bundles used for making reconsolidated bamboo composite. *J Central South Univ For Technol*. 2013;33:153–7. doi:10.14067/j.cnki.1673-923x.2013.10.006 (In Chinese).
30. Zuo YF, Wu YQ, Xiao JH, Li XJ, Long KQ. Effect of preparation technology on mechanical properties of reconstituted bamboo. *J Southwest For Univ*. 2016;36:132–6. doi:10.11929/j.jssn.2095-1914.2016.02.022 (In Chinese).
31. Dai N. Effect of hot-pressing process on the properties of recombined bamboo boards. *ForMach Woodworking Equip*. 2012;40:32–6. doi:10.3969/j.jssn.2095-2953.2012.05.010.
32. Li Q, Wang KH, Yang WM, Hua XQ, Weng FJ, He J. Research on technology of remaking bamboo glued board. *J Bamboo Res*. 2003;22:56–60. doi:10.3969/j.jssn.1000-6567.2003.
33. Lin H. Research on the key techniques of recombined bamboo materials based on *Phyllostachys edulis*. *World Bamboo Rattan*. 2017;15:19–22. doi:10.13640/j.cnki.wbr.2017.03.004.
34. Wang J, Lv Y, Huang C, Ni YH, Song JG. Design of control system of automatic bamboo scrimber cold pressing unit. *J For Eng*. 2017;2(5):95–101. doi:10.13360/j.jssn.2096-1359.2017.05.017.
35. Gong Z, Yuan SF, Wang HY, Zhang J, Li Q. Design of feeding operation from cold press automatic production line for bamboo scrimber. *J Zhejiang For Sci Technol*. 2019;39(6):92–9. doi:10.3969/j.jssn.10013776.2019.06.015.
36. Yu W. Current situation and opportunities for the development of bamboo scrimber industry in China. *World Bamboo Rattan*. 2019;17:1–4. doi:10.13640/j.cnki.wbr.2019.03.001.

37. Sharma B, Gatóo A, Bock M, Mulligan H, Ramage M. Engineered bamboo: state of the art. *Proc Inst Civil Eng-Construct Mat.* 2015;168(2):57–67. doi:10.1680/coma.14.00020.
38. Guan M, Zhu Y, Zhang X. Comparison of bending properties of scrimber and bamboo scrimber. *J Northeast For Univ.* 2006;34(4):7 (In Chinese).
39. Yang Z, Hu Y, Qiu X. Study on bending properties of recombinant bamboo and glued bamboo. *IOP Conf Series: Mat Sci Eng.* 2020;768:32029. doi:10.1088/1757-899X/768/3/.
40. Xu M, Cui ZY, Chen ZF, Xiang JH. The charring rate and charring depth of bamboo scrimber exposed to a standard fire. *Fire Mater.* 2018;42:750–9. doi:10.1002/fam.2629.
41. Cui ZY, Xu M, Chen ZF, Xiang JH. Experimental study on thermal performance of bamboo scrimber at elevated temperatures. *Constr Build Mater.* 2018;182:178–87. doi:10.1016/j.conbuildmat.2018.06.124.
42. Tang XY, Guan MJ, Xu XJ, Yong C. Effect of ultrasonic-antibacterial paraffin treatment on the antifungal performance of bamboo. *J For Eng.* 2022;7(1):45–51. doi:10.13360/j.issn.2096-1359.202103045.
43. Schmidt G, Stute T, Lenz MT, Melcher E, Ressel JB. Fungal deterioration of a novel scrimber composite made from industrially heat treated African highland bamboo. *Ind Crops Prod.* 2020;147:112225. doi:10.1016/j.indcrop.2020.112.
44. Yang LT, Lou ZC, Han X, Liu J, Wang ZS, Zhang Y, et al. Fabrication of a novel magnetic reconstituted bamboo with mildew resistance properties. *Mater Today Commun.* 2020;23:101086. doi:10.1016/j.mtcomm.2020.101086.
45. Wu ZZ, Huang DB, Wei W, Wang W, Wang XD, Wei Q, et al. Mesoporous aluminosilicate improves mildew resistance of bamboo scrimber with CuBP anti-mildew agents. *J Clean Prod.* 2019;209:273–82. doi:10.1016/j.jclepro.2018.10.168.
46. Zhang JZ, Zhou XW, Ren HQ, Zhao RJ. Study on compressive and tensile properties of recombinant bamboo. In: *Proceedings of the 55th International Convention of Society of Wood Science and Technology; 2012; Beijing, China.*
47. Li P. Experimental study on mechanical properties of Bamboo scrimber. *J Hunan Univ Arts Sci (Sci Technol).* 2018;30:53–7. doi:10.3969/j.issn.1672-6146.2018.02.013.
48. Li HT, Zhang HZ, Qiu ZY, Su JW, Wei DD, Lorenzo R. Mechanical properties and stress strain relationship models for bamboo scrimber. *J Renew Mater.* 2020;8:13–27. doi:10.32604/jrm.2020.09341.
49. Wei Y, Ji XW, Duan MJ, Zhao LL, Li GF. Model for axial stress-strain relationship of bamboo scrimber. *Acta Materiae Compositae Sinica.* 2018;35:572–9. doi:10.13801/j.cnki.fhclxb.20170608.002.
50. Sharma B, Gatóo A, Bock M, Ramage M. Engineered bamboo for structural applications. *Constr Build Mater.* 2015;81:66–73. doi:10.1016/j.conbuildmat.2015.01.077.
51. Li HT, Su JW, Wei DD, Zhang QS, Chen G. Comparison study on parallel bamboo strand lumber under axial compression for different directions based on the large scale. *J Zhengzhou Univ (Eng Sci).* 2016;37:67–72. doi:10.3969/j.issn.1671-6833.201412053 (In Chinese).
52. Chen S, Wei Y, Zhao KP, Hang C, Zhao K. Creep performance and prediction model of bamboo scrimber under compression. *Acta Materiae Compositae Sinica.* 2021;38:944–52. doi:10.13801/j.cnki.fhclxb.2020.
53. Wei Y, Zhao KP, Hang C, Chen S, Ding MM. Experimental study on the creep behavior of recombinant bamboo. *J Renew Mater.* 2020;8:251–74. doi:10.32604/jrm.2020.08779.
54. Li YS, Zhang XH, Wu PZ, Zhang JL, Zhao ZL. Creep behavior of bamboo scrimber under long-term load. *J Build Mater.* 2019;22:65–71. doi:10.3969/j.issn.1007-9629.2019.01.010.
55. Kumar A, Vlach T, Laiblova L, Hroudá M, Kasal B, Tywoniak J, et al. Engineered bamboo scrimber: influence of density on the mechanical and water absorption properties. *Constr Build Mater.* 2016;127:815–27. doi:10.1016/j.conbuildmat.2016.10.069.
56. Wang XY, Zhong Y, Luo XY, Ren HQ. Compressive failure mechanism of structural bamboo scrimber. *Polymers.* 2021;13(23):4223. doi:10.3390/polym13234223.

57. Li XZ, Mou QY, Ji SY, Li XJ, Chen ZJ, Yuan G. Effect of elevated temperature on physical and mechanical properties of engineered bamboo composites. *Ind Crops Prod.* 2022;189:115847. doi:10.1016/j.indcrop.2022.115847.
58. Sylvayanti SP, Nugroho N, Bahtiar ET. Bamboo Scrimber's physical and mechanical properties in comparison to four structural timber species. *Forests.* 2023;14(1):146. doi:10.3390/f14010146.
59. Wu MT, Mei LD, Guo N, Ren J, Zhang YN, Zhao Y. Mechanical properties and failure mechanisms of engineering bamboo scrimber. *Constr Build Mater.* 2022;344:128082. doi:10.1016/j.conbuildmat.2022.128082.
60. Chen S, Wei Y, Hu YF, Zhai ZX, Wang LB. Behavior and strength of rectangular bamboo scrimber columns with shape and slenderness effects. *Mater Today Commun.* 2020;25:1–19. doi:10.1016/j.mtcomm.2020.101392.
61. Rao F, Zhu XG, Zhang YH, Ji YH, Lei WC, Li N, et al. Water resistance and mechanical properties of bamboo scrimber composite made from different units of *Bambusa chungii* as a function of resin content. *Constr Build Mater.* 2022;335:127250. doi:10.1016/j.conbuildmat.2022.127250.
62. Sewar YY, Zhang ZC, Meng XM, Wahan MY, Qi HX, Al-Shami QM, et al. Mechanical properties and constitutive relationship of the high-durable parallel strand bamboo. *J Renew Mater.* 2022;10(1):219–35. doi:10.32604/jrm.2022.016013.
63. Hu Y, Xiong LY, Li YB, Semple K, Nasir V, Pineda H, et al. Manufacturing and characterization of wide-bundle bamboo scrimber: a comparison with other engineered bamboo composites. *Materials.* 2022;15(21):7518. doi:10.3390/ma15217518.
64. Zheng YB, Zhou CD, Wang YQ, Zhang P. Strength design values of high-performance bamboo-based composite materials based on reliability requirements. *Constr Build Mater.* 2023;368:130454. doi:10.1016/j.conbuildmat.2023.130454.
65. Wu FY, Wei Y, Lin Y, Zhao K, Huang LJ. Experimental study of bamboo scrimber-filled steel tube columns under axial compression. *Eng Struct.* 2023;280:115669. doi:10.1016/j.engstruct.2023.115669.
66. Yu JB, Yang DY, He Q, Du BC, Zhang SJ, Hu M. Strong, durable and fire-resistant glass fiber-reinforced bamboo scrimber. *Ind Crops Prod.* 2022;181:114783. doi:10.1016/j.indcrop.2022.114783.
67. Chen BW, Liu YQ, Lv WL, Liu CC. Research on the mechanical properties of reconsolidated bamboo column under long term axial compression. *Sichuan Build Sci.* 2019;45:27–31. doi:10.19794/j.cnki.1008 (In Chinese).
68. Rao F, Ji YH, Li N, Zhang YH, Chen YH, Yu WJ. Outdoor bamboo-fiber-reinforced composite: influence of resin content on water resistance and mechanical properties. *Constr Build Mater.* 2020;261:120022. doi:10.1016/j.conbuildmat.2020.12.
69. Li HT, Qiu ZY, Wu G, Wei DD, Lorenzo R, Yuan C, et al. Compression behaviors of parallel bamboo strand lumber under static loading. *J Renew Mater.* 2019;7:583–600. doi:10.32604/jrm.2019.07592.
70. Wei Y, Tang SF, Ji XW, Zhao K, Li GF. Stress-strain behavior and model of bamboo scrimber under cyclic axial compression. *Eng Struct.* 2020;209:110279. doi:10.1016/j.engstruct.2020.110279.
71. Shangguan WW, Zhong Y, Xing XT, Zhao RJ, Ren HQ. Strength models of bamboo scrimber for compressive properties. *J Wood Sci.* 2015;61:120–7. doi:10.1007/s10086-014-1444-9.
72. Xu M, Cui ZY, Chen ZF, Xiang JH. Experimental study on compressive and tensile properties of a bamboo scrimber at elevated temperatures. *Constr Build Mater.* 2017;151:732–41. doi:10.1016/j.conbuildmat.2017.06.128.
73. Huang DS, Bian YL, Zhou AP, Sheng BL. Experimental study on stress-strain relationships and failure mechanisms of parallel strand bamboo made from phyllostachys. *Constr Build Mater.* 2015;77:130–8. doi:10.1016/j.conbuildmat.2014.12.012.
74. Yang YQ, Fahmy MFM, Pan ZH, Zhan Y, Wang RH, Wang B, et al. Experimental study on basic mechanical properties of new BFRP-bamboo sandwich structure. *Constr Build Mater.* 2020;264:120642. doi:10.1016/j.conbuildmat.2020.120642.
75. Zhao P, Zhang X. Size effect of section on ultimate compressive strength parallel to grain of structural bamboo scrimber. *Constr Build Mater.* 2019;200:586–90. doi:10.1016/j.conbuild.

76. Rao F, Ji YH, Huang YX, Li N, Zhang YH, Chen Y, et al. Influence of resin molecular weight on bonding interface, water resistance, and mechanical properties of bamboo scrimber composite. *Constr Build Mater.* 2021;292:123458. doi:10.1016/j.conbuildmat.2021.123458.
77. Sun YH, Yu WJ, Wei XX, Ge LJ, Guo ZW, Zhang Y. Bamboo strand-based structural composite lumber: influence of technological parameters on physico-mechanical properties. *Constr Build Mater.* 2021;271:121795. doi:10.1016/j.conbuildmat.2020.121795.
78. Liu CM, Wu XZ, Li XJ, Wu YQ. Investigation into the effects of various processing treatments on the flexural performance of carbon fiber reinforced polymer-bamboo scrimber composites. *Aust J Struct Eng.* 2022;23(4):370–86. doi:10.1080/13287982.2022.2073954.
79. Chen S, Wei Y, Zhu J, Lin Y, Du H. Experimental investigation of the shear performance of bamboo scrimber beams reinforced with bamboo pins. *Constr Build Mater.* 2023;365:130044. doi:10.1016/j.conbuildmat.2022.130044.
80. Qiu ZY, Wang JX, He HG, Fan HL. First-order anisotropic beam model and failure criterion for flexural parallel bamboo strand lumbers. *Constr Build Mater.* 2020;263:120125. doi:10.1016/j.conbuildmat.2020.120125.
81. Zhao JB, Meng ZX, Jin Z, Chen D, Wu YS, Zhang W. Bending properties of bamboo scrimber with holes in different sizes and positions. *Constr Build Mater.* 2019;200:209–17. doi:10.1016/j.conbuildmat.2018.12.076.
82. Zou Z, Wu J, Zhang X. Influence of moisture content on mechanical properties of bamboo scrimber. *J Mater Civ Eng.* 2019;31:6019004. doi:10.1061/(ASCE)MT.1943-5533.0002746.
83. Wu XZ, Huang XY, Li XJ, Wu YQ. Flexural performance of CFRP-bamboo scrimber composite beams. *J Renew Mater.* 2019;7:1295–307. doi:10.32604/jrm.2019.07839.
84. Yu YL, Liu R, Huang YX, Meng FD, Yu WJ. Preparation, physical, mechanical, and interfacial morphological properties of engineered bamboo scrimber. *Constr Build Mater.* 2017;157:1032–9. doi:10.1016/j.conbuildmat.2017.09.185.
85. Yang D, Li HT, Wei DD, Lorenzo R, Corbi I, Corbi O, et al. Length effect on bending properties and evaluation of shear modulus of parallel bamboo strand lumber. *Eur J Wood Wood Prod.* 2021;79:1507–17. doi:10.1007/s00107-021-01714-1.
86. Qiu Z, Wang J, Fan H. Low velocity flexural impact behaviors of bamboo fiber reinforced composite beams. *Polym Test.* 2021;94:107047. doi:10.1016/j.polymertesting.2020.107047.
87. Qiu Z, Wang J, Fan H. Impact bending behaviors of parallel bamboo strand lumber beams: velocity sensitivity and anisotropy. *Compos Struct.* 2021;263:113711. doi:10.1016/j.compstruct.2021.113711.
88. Wang XY, Luo XY, Ren HQ, Zhong Y. Bending failure mechanism of bamboo scrimber. *Constr Build Mater.* 2022;326:126892. doi:10.1016/j.conbuildmat.2022.126892.
89. Wang MT, Cai XF, Lu YB, Noori A, Chen FM, Chen B, et al. Tensile mechanical properties and failure mechanism of bamboo scrimber under different strain rates. *Constr Build Mater.* 2021;299:124258. doi:10.1016/j.conbuildmat.2021.124.
90. Luo XY, Wang XY, Ren HQ, Zhang SB, Zhong Y. Long-term mechanical properties of bamboo scrimber. *Constr Build Mater.* 2022;338:127659. doi:10.1016/j.conbuildmat.2022.127659.
91. Luo XY, Luo XQ, Ren HQ, Zhang SB, Zhong Y. The long-term mechanical properties of BS perpendicular to the grain. *Polymers.* 2022;15(1):128. doi:10.3390/polym15010128.
92. Cid SCG, Cardoso DCT, de Andrade Silva F, Krause JQ. Influence of hornification on the physical and flexural properties of Moso bamboo. *Constr Build Mater.* 2020;248:118701. doi:10.1016/j.conbuildmat.2020.118701.
93. Yang L, Huang Z. Mould proof treatment technology of bamboo and its effects on mechanical properties in *Neosinocalamus affinis*. *J Bamboo Res.* 2019;38:52–7. doi:10.19560/j.cnki.issn.
94. Chen G, Yu YF, Li X, He B. Mechanical behavior of laminated bamboo lumber for structural application: an experimental investigation. *Eur J Wood Wood Prod.* 2020;78:53–63. doi:10.1007/s00107-019-01486-9.
95. Appiah-Kubi E, Awotwe-Mensah M, Mitchual SJ. Assessment of physical and mechanical properties of juvenile and matured *Bambusa vulgaris* glue-laminated bamboo for structural applications in Ghana. *Sustain Struct.* 2023;3(2):26. doi:10.54113/j.sust.2023.000026.

96. Sousa HS, Branco JM, Lourenço PB. Glulam mechanical characterization. *Mater Sci Forum*. 2013;730:994–9. doi:10.4028/www.scientific.net/MSF.730-732.994.
97. Hugot F, Cazaurang G. Mechanical properties of an extruded wood plastic composite. *Mech Ind*. 2009;10:519–24. doi:10.1051/meca/2010010.
98. Verma CS, Sharma NK, Chariar VM, Maheshwari S, Hada MK. Comparative study of mechanical properties of bamboo laminae and their laminates with woods and wood based composites. *Compos Part B: Eng*. 2014;60:523–30. doi:10.1016/j.composi.
99. Ross RJ. *Wood handbook: wood as an engineering material*. Madison, WI: USDA Forest Service, Forest Products Laboratory; 2010. doi:10.2737/FPL-GTR-190.
100. Dong ZQ, Ji JH, Liu ZQ, Wu C, Wu G, Zhu H, et al. I-shaped ECC/UHPC composite beams reinforced with steel bars and BFRP sheets. *Sustain Struct*. 2023;3(1):22. doi:10.54113/j.sust.2023.000022.
101. Zeng JJ, Duan ZJ, Gao WY, Bai YL, Ouyang LJ. Compressive behavior of FRP-wrapped seawater sea-sand concrete with a square cross-section. *Constr Build Mater*. 2020;262:120881. doi:10.1016/j.conbuildmat.2020.120881.
102. Liao JJ, Yang KY, Zeng JJ, Quach WM, Ye YY, Zhang L. Compressive behavior of FRP-confined ultra-high performance concrete (UHPC) in circular columns. *Eng Struct*. 2021;249:113246. doi:10.1016/j.engstruct.2021.113246.
103. Verma CS, Chariar VM. Development of layered laminate bamboo composite and their mechanical properties. *Compos Part B: Eng*. 2012;43:1063–9. doi:10.1016/j.compositesb.2011.11.065.
104. Marx CM, Moody RC. *Bending strength of shallow glued-laminated beams of a uniform grade*. United States Department of Agriculture; 1981.
105. Zhang XL, Que YL, Wang XM, Li ZR, Zhang LL, Han C, et al. Experimental behavior of laminated veneer lumber with round holes, with and without reinforcement. *BioResources*. 2018;13:8899–910. doi:10.15376/biores.13.4.8899-8910.
106. Ni L, Zhang XB, Liu HR, Sun ZJ, Song GN, Yang L, et al. Manufacture and mechanical properties of glued bamboo laminates. *BioResources*. 2016;11:4459–71. doi:10.15376/biores.11.2.4459-4471.
107. Li Z, Zhang JY, Wang R, Monti G, Xiao Y. Design embedment strength of plybamboo panels used for GluBam. *J Mater Civ Eng*. 2020;32(5):04020082. doi:10.1061/(ASCE)MT.1943-5533.0003128.
108. Wang BJ, Chui YH. Manufacturing of LVL using cost-effective resin impregnation and layup technologies. *Wood Sci Technol*. 2012;46:1043–59. doi:10.1007/s00226-012-0465-z.
109. Zhang H, Li HT, Li YJ, Xiong ZH, Zhang NN, Lorenzo R, et al. Effect of nodes on mechanical properties and microstructure of laminated bamboo lumber units. *Constr Build Mater*. 2021;304:124427. doi:10.1016/j.conbuildmat.2021.124427.
110. Zhou J, Feng X, Zhou X. Experimental research on mechanical properties of larch glulam. *J Cent South Univ For Technol*. 2016;36(8):125–9. doi:10.14067/j.cnki.1673-923x.2016.08.022.
111. Kretschmann DE. *Mechanical properties of wood*. In: *Wood handbook: wood as an engineering material*. Madison, Wisconsin; 2010.